Journal of Controlled Release 370 (2024) 182–194

Contents lists available at ScienceDirect

Journal of Controlled Release

journal homepage: www.elsevier.com/locate/jconrel

Can *in vitro/in silico* tools improve colonic concentration estimations for oral extended-release formulations? A case study with upadacitinib

Alessia Favaron [a], Bart Hens [b,*], Maiara Camotti Montanha [b], Mark McAllister [b], Irena Tomaszewska [b], Shaimaa Moustafa [b], Marília Alvarenga de Oliveira [b], Abdul W. Basit [a,**], Mine Orlu [a,**]

[a] *UCL School of Pharmacy, University College London, London WC1N 1AX, UK.*
[b] *Drug Product Design, Pfizer, Sandwich, Kent CT13 9NJ, United Kingdom*

ARTICLE INFO

Keywords:
Colonic targeting
Oral drug delivery
Rinvoq
Upadacitinib
Modeling
Dissolution

ABSTRACT

Upadacitinib, classified as a highly soluble drug, is commercially marketed as RINVOQ®, a modified-release formulation incorporating hydroxypropyl methylcellulose as a matrix system to target extended release throughout the gastrointestinal (GI) tract. Our study aimed to explore how drug release will occur throughout the GI tract using a plethora of *in vitro* and *in silico* tools. We built a Physiologically-Based Pharmacokinetic (PBPK) model in GastroPlus™ to predict the systemic concentrations of the drug when administered using *in vitro* dissolution profiles as input to drive luminal dissolution. A series of *in vitro* dissolution experiments were gathered using the USP Apparatus I, III and IV in presence of biorelevant media, simulating both fasted and fed state conditions. A key outcome from the current study was to establish an *in vitro-in vivo* correlation (IVIVC) between (i) the dissolution profiles obtained from the USP I, III and IV methods and (ii) the fraction absorbed of drug as deconvoluted from the plasma concentration-time profile of the drug. When linking the fraction dissolved as measured in the USP IV model, a Level A IVIVC was established. Moreover, when using the different dissolution profiles as input for PBPK modeling, it was also observed that predictions for plasma C_{max} and AUC were most accurate for USP IV compared to the other models (based on predicted *versus* observed ratios). Furthermore, the PBPK model has the utility to extract the predicted concentrations at the level of the colon which can be of utmost interest when working with specific *in vitro* assays.

1. Introduction

Upadacitinib is a selective JAK1 inhibitor, marketed as the modified-release (MR) drug product RINVOQ® [1]. As well as being used in the treatment of rheumatoid arthritis and dermatitis, upadacitinib is approved for inflammatory bowel disease (IBD), specifically for the treatment of patients with moderately to severely acute ulcerative colitis (UC) or Crohn's disease (CD) [1]. RINVOQ® is marketed in three dosages 15, 30, and 45 mg, in an MR monolithic formulation made of hydroxypropyl lmethylcellulose (HPMC). Upon administration, water in the gastrointestinal (GI) fluids penetrates the system: swelling, diffusion, and erosion fronts develop, allowing the gradual controlled release of the drug from the polymer matrix [2].

MR formulations represent a commonly used technology for drugs to reach different regions of the GI tract [3]. The European Medicines Agency (EMA) guidelines for the approval of these specific formulations require information on the therapeutic objective and rationale of the product, pharmacokinetic characteristics of the active substance, information on the formulation excipients, and release mechanism from the product [4]. However, specifically for MR formulations, there are no well-established and accepted *in vitro* or *in vivo* techniques to assess the bioavailability of the drug in each specific part of the intestine. The standard method for bioavailability assessment only relies on the systemic plasma drug concentration instead of drug availability at the site of action. This approximation, for those drugs with local therapeutic action, is inappropriate since molecules reach the site of action before entering the systemic circulation, and even more, for low permeable drugs, plasma concentration is a suboptimal indicator of what happens

* Correspondence to: Drug Product Design, Pfizer, Discovery Park, Ramsgate Road, Sandwich CT13 9ND, UK.
** Corresponding authors at: UCL School of Pharmacy, 29-39 Brunswick Square, London WC1N 1AX, UK.
E-mail addresses: bart.hens@pfizer.com (B. Hens), a.basit@ucl.ac.uk (A.W. Basit), m.orlu@ucl.ac.uk (M. Orlu).

https://doi.org/10.1016/j.jconrel.2024.04.024
Received 14 December 2023; Received in revised form 12 March 2024; Accepted 12 April 2024
0168-3659/© 2024 The Authors. Published by Elsevier B.V. This is an open access article under the CC BY license (http://creativecommons.org/licenses/by/4.0/).

at the site of action [5]. Documentation of bioavailability and bioequivalency, as indicated by the guideline for locally acting drugs, can be achieved by using acceptable pharmacodynamic endpoints, and/or suitable designed and validated *in vitro* studies [5,6]. Therefore, *in vivo* plasma data should be supplemented with reliable *in vitro* predictive tools that can take into consideration the colonic environment on the one hand, and the physiochemical characteristics of the active substance and formulation on the other.

The most frequently used *in vitro* models to simulate concentrations of drugs are: (i) single-stage United States Pharmacopoeia (USP) I and II (*i.e.,* basket and paddle setup, respectively), the compendial reciprocating cylinder (USP apparatus III) and the flow-through cell apparatus (USP apparatus IV). Specifically, the USP III and IV tools are useful to simulate drug release for MR formulations along the GI tract under both fasted and fed state conditions [7–9]. The advantage of both systems, over conventional USP apparatus (I and II) is the possibility to work with biorelevant media that can be continuously changed during a single experiment, mimicking the transit of the form along the different physiological conditions of the GI tract, for both prandial states.

AbbVie, during the development of RINVOQ®, evaluated the correlation between the fraction dissolved (from a USP I apparatus) from different HPMC formulations and its corresponding fraction absorbed (obtained after deconvolution of the plasma profile). The result was the establishment of a Level A *in vitro-in vivo* correlation (IVIVC) [10]. The first objective of our work was to build upon this foundational Level A IVIVC to incorporate the dissolution data from USP Apparatus III and IV for the establishment of a new IVIVC. In the literature, USP III and IV, through the use of biorelevant media, represent the ideal dissolution apparatus for MR formulations [11,12]. Therefore, this innovative approach allowed us to identify whether USP III and IV with biorelevant media would be superior to the USP I apparatus and whether a new Level A IVIVC could be obtained. This workflow is unique and could provide a template for the pharmaceutical industry in devising new approaches to developing IVIVCs.

As a second objective, we aimed to investigate a plethora of *in vitro* and computational tools that reflect the colonic (patho)physiology to predict the release and concentrations of drugs in the colon from this MR drug product. Physiologically Based Pharmacokinetics (PBPK) analysis is a useful biopharmaceutical modeling tool to predict the rate of absorption and plasma concentration of orally delivered drugs in different GI tract regions, over time. GastroPlus™ is one of the many software packages available today with the ability to combine (i) human or animal gastrointestinal GI physiology, (ii) physicochemical, biopharmaceutics, and PK properties of the drug, and (iii) formulation characteristics to finally predict the *in vivo* performance of the drug in different population settings. Recently, specifically for immediate-release (IR) formulations, increasing confidence in the use of PBPK modeling to predict plasma concentration and luminal concentration of oral drugs has shown good accuracy and predictive performance [13–16]. However, in the case of MR formulations, the *in silico* model requires additional data. While the absorption scale factor can be adjusted to account for regional absorption differences in GastroPlus™, incorporating details about the pharmaceutical dosage form's specific excipient composition or manufacturing process, which may impact the controlled drug release profile *in vivo*, remains challenging. Therefore, predicting the luminal colonic concentrations of such formulations necessitates biopredictive *in vitro* dissolution data. In this work, a PBPK model of RINVOQ® was built and optimized to predict both the systemic and local colonic concentration of upadacitinib. The *in vitro* dissolution data from USP I, III, and IV, were incorporated in the model as a 1st order Weibull function, which takes into account the complexities of formulation release pattern in response to changing media conditions, allowing for a more comprehensive representation of the drug's behavior throughout the GI tract.

Overall, our study aims to demonstrate a streamlined workflow that combines *in vitro* and *in vivo* biopharmaceutical data, highlighting their potential for industry use and regulatory interaction. The primary aim of this study is to establish a workflow for the pharmaceutical industry, demonstrating the efficacy of combining *in vitro* dissolution models and *in silico* simulations to evaluate the bioperformance of an oral drug product. As a complementary objective, the study also seeks to ascertain upadacitinib concentrations in the colon.

1.1. Materials

Upadacitinib (98.56%) was received from MedChem Express (Cambridge Bioscience, UK). RINVOQ® 30 mg extended-release tablet was distributed by AbbVie Inc. (Chicago, Illinois, USA). All reagents were of analytical grade. FaSSIF/FeSSIF/FaSSGF powder, FaSSIF-V2/FeSSIF-V2 powder, FaSSCoF/FeSSCoF powder were obtained from Biorelevant (London, UK) and media were prepared following the shared protocols by the distributer. Lipofundin® MCT 20, an o/w emulsion used for parental nutrition, was purchased from Braun Melsungen A.G. (Melsungen, Germany). The experiment was performed with a Level II biorelevant media that simulate the composition and pH of the different gastrointestinal tract compartments. The media compositions are reported in Tables 1 (fasted media) and 2 (fed media) below.

2. Methods

2.1. Dissolution data

To improve the *in silico* prediction of upadacitinib release from the extended-release formulation, three dissolution profiles were implemented into the PBPK model:

2.1.1. USP apparatus I

USP apparatus I experiments were conducted by AbbVie as reported in literature [10,17]: apparatus USP I with basket, using dissolution media of 0.05 M phosphate buffer at pH 6.8, rotational speed of 100 rotations per minute (rpm).

2.1.2. USP apparatus III

The USP apparatus III (reciprocating cylinder) experiments were performed using the following protocol. RINVOQ® is a hypromellose monolithic dosage form. Due to the high solubility in acidic conditions,

Table 1
Fasted Biorelevant media Level II compositions. [1] made with Phares SIF powder, [2] made with Phares FaSSIF-V2 powder, [3] made with Phares FaSSIF-V2 powder, [4] made with Phares SIF powder.

Fasted media	FaSSGF[1]	FaSSIF-V2[2]	FaSSIF midgut[3]	SIFileum[4]	FaSSCoF
Sodium taurocholate (mM)	0.08	3	1.5	0.8	–
Lecithin (mM)	0.02	0.2	0.1	0.2	0.3
Sodium cholate (mM)	–	–	–	–	0.153
HCl	qs pH 1.6	–	–	–	–
NaOH (mM)	–	34.8	36.5	105	120
Sodium oleate (mM)	–	–	–	–	0.14
Maleic acid (mM)	–	19.1	19.3	52.8	75.8
Sodium chloride (mM)	34.2	68.6	76.1	30.1	–
Tris (mM)	–	–	–	–	45.4
Osmolality (mOsm/kg)	121	180	190	190	196
Buffer capacity [(mmol/L)/ ΔpH]	n.a.	10	10	10	16
pH	1.6	6.5	6.8	**8**	7.8

Table 2
Fed state biorelevant media composition. [5] made with Phares FaSSIF-V2 powder and SIF powder, [6] made with Phares FaSSIF-V2 powder and SIF powder, [7] made with Phares SIF powder.

Fed media	$FeSSGF_{early}$	$FeSSGF_{middle}$	$FeSSGF_{late}$	FeSSIF-V2[5]	FeSSIF [6] $_{midgut}$	SIF^{7}_{ileum}	FeSSCoF
Maleic acid (mM)	47.0	–	–	–	–	–	–
Acetic acid (mM)	–	18.31	–	–	–	–	–
Sodium acetate (mM)	–	32.98	–	–	–	–	–
Ortho-phosphoric acid (mM)	–	–	5.5	–	–	–	–
Sodium dihydrogen phosphate (mM)	–	–	32	–	–	–	–
Lipofundin/buffer	17.5: 82.5	8.75: 91.25	4.375: 95.625	–	–	–	–
HCl/NaOH	qs pH 6.4	qs pH 5	qs pH 3	–	–	–	–
Sodium chloride (mM)	270.1	181.7	127.5	–	–	–	–
Sodium taurocholate (mM)	–	–	–	10	5	0.8	–
Sodium cholate (mM)	–	–	–	–	–	–	0.6[2]
Lecithin (mM)	–	–	–	2	1	0.2	0.5
Glyceryl monooleate (mM)	–	–	–	5	2.5	–	–
Sodium oleate (mM)	–	–	–	0.8	0.4	–	0.2[3]
Glucose (mg/mL)	–	–	–	–	–	–	14
Tris (mM)	–	–	–	–	–	–	30.5
Maleic acid (mM)	–	–	–	71.9	46.5	52.8	30.15
NaOH (mM)	–	–	–	102.4	83	105	16.5
Sodium chloride (mM)	–	–	–	125.5	102.6	30.1	34
Osmolality (mOsm/kg)	559	400	300	390	300	190	207
Buffer capacity (HCl) [(mmol/L)/ΔpH]	21.33	25	25	25	25	10	15
pH	6.4	5	3	6.5	6.8	8.0	6.0

and to the characteristics of the cellulose coating of the tablet, the release of the API from the form is expected to occur already in the stomach, and along the entire GI tract. For this reason, the dissolution test was performed over a 9 h experiment in biorelevant media. Six tablets were tested simultaneously ($n = 6$) at 37 ± 0.5 °C. Table 3 gives the time points when a switch in media occurred to represent the GI transit in a biorelevant manner. Samples were drawn manually from the vessel and each vessel had a volume of 235 mL of media. PTFE 1 μm (polytetrafluorethylene, Whatman Rezist, Whatman, USA) was used to filter all samples prior to HPLC analysis. In our protocol, there were specific exceptions for samples from early, middle, and late FeSSGF runs and FaSSIF-V2 when conducted in fed state. These samples were mixed with hydrochloric acid (HCl) in a ratio 1:2 to improve the separation of lipids from the rest of the sample components. Samples were vortexed and centrifuged at 1400 rpm for 10 min. The clear supernatant was then transferred into an HPLC vial and injected into the HPLC system.

2.1.3. USP apparatus IV

RINVOQ® 30 mg dissolution experiments were conducted with the open-loop USP apparatus IV (Flow-through cell). The setting of the experiment is shown in Table 3.

A 5 mm-sized glass bead was placed at the bottom of the cell (22.6 mm ∅) and 1.7 g of 1 mm glass beads were poured on top of the 5 mm bead to homogenously distribute the flow of media reaching the tablet. The tablet was placed on top of the beads, without a holder to avoid constraints on the swelling of the tablet. On top of the cell, where the fluid exiting the cell flows, two MNGF-5 filters (Macherey Nagel Glass Fiber, 0.4 μm pore size, 0.4 mm pore thickness, 25 mm diameter, Macherey-Nagel, Germany) with 0.1 g of glass wool in between, were inserted. Six tablets were tested simultaneously ($n = 6$) at 37 ± 0.5 °C. Samples were collected manually and transferred into an HPLC vial for HPLC analysis. As with the USP apparatus III experiments, samples from $FeSSGF_{early/middle/late}$ and FaSSIF-V2 in fed state run, were transferred in a vial with HCl in the ratio 1:2. Samples were vortexed and centrifuged at 1400 rpm for 10 min. Samples were then filtered with PTFE 1 μm filters into an HPLC vial and injected into the HPLC system. The analytical method for the detection of upadacitinib was the same as used for the experiment with USP apparatus III. Finally, it is an unintended consequence that monolithic dosage forms, due to their size and closure of pylorus, may not promptly exit the stomach postprandially, as gastric emptying can be delayed until the digestion of food is underway. Therefore, it was presumed that the conditions in the small intestine

Table 3
USP III and USP IV protocol, in both fasted and fed state.

GI region	Level 2 Biorelevant Media	Period from beginning of experiment (min)	Duration of exposure	Dip rate (dips/min) in USP III	Flow rate (mL/min) in USP IV	Number of cells/vessels	pH biorelevant media
Fasted state							
Stomach	FaSSGF	0–60	60	12	8	6	1.6
Duodenum	FaSSIF-V2	60–100	40	10	4	6	6.5
Midgut	FaSSIF midgut	100–180	80	10	4	6	6.8
Ileum	SIF ileum	180–240	60	10	4	6	8.0
Ascending colon	FaSSCoF	240–540	300	6	4	6	7.8
Fed state							
	FeSSGF early	0–20	20	8	6	6	6.4
Stomach	FeSSGF middle	20–180	160	8	6	6	5.0
	FeSSGF late	180–240	60	8	6	6	3
Duodenum	FaSSIF-V2	240–280	40	10	4	6	6.5
Midgut	FaSSIF midgut	280–360	80	10	4	6	6.8
Ileum	SIF ileum	360–420	60	10	4	6	8.0
Ascending colon	FeSSCOF	420–540	120	6	4	6	6.0

more closely resembled those of the fasted state rather than the fed state [18]. As a result, dissolution media mimicking the fasted state were employed for both pre-and post-prandial administration experiments, a practice previously established for monolithic drug products [18].

2.2. Quantitative analytical method

Upadacitinib was assayed with an HPLC-UV (1290 Infinity, Agilent Technologies) system using a Poroshell 120 EC – C18 (50 × 3.0 mm, 2.7 mm) column set at the controlled temperature of 45 °C. The mobile phase A consisted of water with 0.1% formic acid, and the mobile phase B of acetonitrile with 0.1% formic acid. The HPLC run was a gradient program, as reported in *Supplementary data*. The flow rate was 0.6 mL/min, with an injection volume of 2 µl, and the wavelength of detection was set at 352 nm. The concentration range linearity was 0.05 µg/mL to 80 µg/mL.

2.3. Similarity factor

After collecting dissolution data, the similarity between the dissolution profiles obtained from USP apparatus I, III, and IV, was assessed using the f2 similarity factor, according to the following equation:

$$f_2 = 50log\left\{\left[1+\frac{1}{n}\sum_{t=1}^{n} w_t(R_t - T_t)^2\right]^{-0.5} \times 100\right\}$$

Where:n = number of time points at which dissolution data were collected.w_t = optional weight factor.R_t = percentage of drug dissolved from the reference assay at time t.T_t = percentage of drug dissolved from the test assay at time point t.

The f2 factor is a widely accepted parameter used to quantitatively compare dissolution profiles and evaluate the similarity between two curves. It takes into account both the mean and the variance of the percentage of drug dissolved at each time point and provides a numerical value that indicates the degree of similarity between the two profiles. A high f2 value (typically ≥50) suggests a high degree of similarity between the two dissolution profiles, indicating that the formulations behave similarly under the different dissolution conditions tested [6,19].

2.4. PBPK model

Simulations were performed by the commercially available PBPK modeling software GastroPlus™ 9.8.3 (Simulations Plus, Inc., Lancaster, CA, USA). All data from model development and verification were sourced from publicly available resources [10,17], as reported in Table 4. Parameters used for PBPK model development (*e.g.,* drug's physicochemical and biopharmaceutics properties) were based on literature data on upadacitinib and are reported in Table 5. Upadacitinib mean concentration-time profiles in the different clinical studies were digitized using PlotDigitizer (PlotDigitizer.com).

Table 4
The PBPK simulations and respective study designs conducted for upadacitinib model development and verification.

#	Study	Subjects	Upadacitinib formulation: Dosing regimen	PBPK model objective
1	M13–548 (ADME)	$n = 4$, healthy	30 mg Oral solution	Development
2	Mohamed et al. [10]	$n = 20$, healthy	IR 24 mg, fasted state	Development
3	Mohamed et al. [10]	$n = 20$, healthy	ER 30 mg, 10, 20, 30% HPMC, fasted state	Verification
4	M15–878	$n = 42$, healthy	ER (ER18) 30 mg fasted state	Verification
5	M15–878	$n = 42$, healthy	ER (ER18) 30 mg fed state	Verification
6	M14–680	$n = 12$, healthy	ER (ER8) 30 mg fasted state	Verification
7	M14–680	$n = 12$, healthy	ER (ER8) 30 mg fed state	Verification

To define the absorption of upadacitinib from the oral forms, the Advanced Compartmental Absorption Transit (ACAT) model was used, which defines the transit, absorption, and secretion of intestinal fluid volumes [20] throughout 9 anatomic compartments, from the stomach to the ascending colon. ACAT was applied to all simulations with the stomach transit time (STT) adjusted for both fasted and fed states. Specifically, the fed states used in this study were two, which differentiated only for the STT: Fed State [1] with a STT of 1h30min, Fed State [2] with a STT of 2h30min. Fasted state STT was adjusted to 1h20min. To describe the distribution and elimination of upadacitinib, a 2-compartmental pharmacokinetic model was applied to describe the clearance and volume of distribution (PKPLus v2.5 model, Simulations Plus, Inc., Lancaster, CA, USA). Specifically, the parameters of volume of distribution and clearance were calculated from the systemic data of 24 mg RINVOQ®, immediate release capsule [10]. Upadacitinib is cleared *via* both urine and feces, and unchanged upadacitinib is the major moiety in plasma (79%), with only <13% of related metabolites. The cytochrome (CYP) P450, CYP3A4, and CYP2D6 can all metabolize upadacitinib, although they have no significant effect on the drug's PK.

The study design, including the dose, route of administration, and study duration, matched the clinical study design for each specific study, as outlined in Table 4. Model-predicted parameters, including plasma C_{max}, T_{max}, $AUC_{0\text{-}t}$, and AUC_{inf}, were compared to the corresponding observed upadacitinib exposures from the clinical trials. The simulations were conducted on the same number of subjects as the relative *in vivo* study. To assess the predictive performance of the model, Average Absolute Fold Error (AAFE), defined as the average of the absolute values of the fold difference between predicted and observed PK parameters across all subjects, was used. An AAFE value of 2-fold or less was established as the threshold for acceptable model performance.

$$0.5 \leq \frac{\text{Predicted PK Parameter}}{\text{Observed PK Parameter}} \leq 2$$

Conversely, an AAFE value of 1.25-fold or lower was indicative of good model performance, reflecting a tighter concordance between the predicted and observed PK parameters [21].

2.5. In vitro-in vivo correlation (IVIVC)

To develop a Level A *In vitro-in vivo* correlation (IVIVC), we began by collecting essential data from multiple sources. Fraction-absorbed (Fa) data from a clinical study conducted by AbbVie Inc. in healthy patients [10] was digitized at specific time intervals 0, 1, 2, 4, 6, 8 h and utilized (PlotDigitizer.com). Dissolution data (Fdiss) extracted from USP apparatus I, USP apparatus III, and USP apparatus IV, were incorporated at the same time intervals as the Fa. The integration process involved aligning the digitized *in vivo* absorption data (Fa) with the three corresponding *in vitro* dissolution data for each USP apparatus (Fdiss), generating individual Levy Plots. To evaluate the predictive performance of each USP apparatus, we calculated internal prediction errors. These were calculated by juxtaposing the observed *in vivo* dissolution outcomes for each apparatus against their corresponding values projected by the regression model. The percentage prediction error (%PE) was derived using the formula:

$$\%PE = \frac{\text{Observed } in\ vivo \text{ data} - \text{Predicted } in\ vitro \text{ data}}{\text{Observed } in\ vivo \text{ data}}\ x\ 100$$

Subsequently, the mean %PE across all apparatuses was calculated, accompanied by the standard deviation.

Table 5
Upadacitinib physicochemical and biopharmaceutics properties for model development.

Physicochemical parameters	Value	Reference
Compound name (PF)	RINVOQ® 30 mg	
API name (PF)	Upadacitinib hemihydrate	
Molecular weight (g/mol)	380.4 Upadacitinib	https://www.ema.europa.eu/en/documents/assessment-report/rinvoq-epar-public-assessment-report_en.pdf
pKa(s) (basic / acidic)	12.8 (amide nitrogen) 4.7 (nitrogen of the imidazole)	https://www.ema.europa.eu/en/documents/assessment-report/rinvoq-epar-public-assessment-report_en.pdf
LogP	2.50	Rinvoq, INN-upadacitinib (europa.eu)
LogD (at which pH)	2.50 (pH 7)	Rinvoq, INN-upadacitinib (europa.eu)
Blood:Plasma Ratio	1	Rinvoq, INN-Upadacitinib (europa.eu)
Fraction unbound in plasma (Fu)	At 1 μM - 0.48	Rinvoq, INN-upadacitinib (europa.eu)
Acid or Base	Weak base	
Absorption related parameters		
Peff in humans (cm/s x 10e4), predicted using Mech Peff model	10.2	https://www.accessdata.fda.gov/drugsatfda_docs/nda/2019/211675Orig1s000ClinPharmR.pdf
Aqueous solubility at different pH values (mg/mL)		
0.1 N HCl5454	38.4 ± 1.5	Product Quality Review (s) (fda.gov)
50 mM phosphate buffer (pH 2–3)	10.5 ± 0.1	Product Quality Review (s) (fda.gov)
50 mM citrate buffer (pH 3–3.39)	4.48 ± 0.08	Product Quality Review (s) (fda.gov)
50 mM citrate buffer (4–4.16)	1.00 ± 0.01	Product Quality Review (s) (fda.gov)
50 mM citrate buffer (pH 5)	0.289 ± 0.006	Product Quality Review (s) (fda.gov)
50 mM citrate buffer (pH 6–5.9)	0.196 ± 0.001	Product Quality Review (s) (fda.gov)
50 mM phosphate buffer (pH 7–7.14)	0.194 ± 0.001	Product Quality Review (s) (fda.gov)
50 mM phosphate buffer (pH 8–7.9)	0.200 ± 0.013	Product Quality Review (s) (fda.gov)
50 mM phosphate buffer (pH 9–9.11)	0.199 ± 0.006	Product Quality Review (s) (fda.gov)
Biorelevant solubility (mg/mL)		
FaSSIF (pH 6.5)	0.262 ± 0.003	Product Quality Review (s) (fda.gov)
FeSSIF (pH 5)	0.455 ± 0.006	Product Quality Review (s) (fda.gov)
Transporter and/or metabolism interference	Substrate of CYP3A4 (and CYP2A6 in minor concentration) / P-gp and BCRP	https://www.accessdata.fda.gov/drugsatfda_docs/nda/2019/211675Orig1s000ClinPharmR.pdf
Crystalline form	Yes	Rinvoq, INN-upadacitinib (europa.eu)
Systemic compartmental pharmacokinetics parameters (calculated from the systemic data of 24 mg RINVOQ®, immediate release capsule).		
CL (L/h)	47.413	
Vc (L/kg)	0.34503	
T1/2 (h)	4.69	
k12	0.44656	
k21	0.18422	
V2	0.83637	

3. Results and discussion

To assess the release of upadacitinib throughout the GI tract and estimate the concentration of the active ingredient reaching the large intestine, and consequently, its availability for absorption, a study with multiple *in vitro* dissolution models was performed and the generated dissolution profiles were applied as the input for the constructed PBPK model. Afterward, the predicted plasma profile of upadacitinib was compared with the clinical data and the best prediction can be assigned by the IVIVC analysis for each *in vitro* release profile *versus* fraction absorbed.

3.1. USP apparatus impact on the dissolution of RINVOQ® ER tablet

Mohamed et al. evaluated the *in vitro* drug release profile of four upadacitinib extended-release formulations with different percentages of HPMC [10]. The formulation which contained 20% HPMC was the prototype for the planned commercial formulation. In their selected method (USP I at pH 6.8), the formulation released about 95% of the active drug at 24 h, and 80% at 9 h as shown in Fig. 1A. This dissolution profile was successful in establishing a predictive Level A linear IVIVC correlation for RINVOQ® ER formulation, thus it was chosen in our study as the reference drug-release profile.

In the fasted state experiments, the drug release assessment was conducted within a 9-h timeframe using five distinct biorelevant media. In Fig. 1B, USP apparatus III revealed a total drug release from the matrix, with an average recovery of 106.6% at the end of the experiment. Interestingly, during the initial 60 min of the experiment conducted in FaSSGF with a pH of 1.6, a significant release of 45.64% of the drug from the matrix was observed. This trend nearly doubled the comparative drug release profile observed with USP Apparatus I. These findings collectively indicate that USP Apparatus III, in this context, notably overestimated the release of upadacitinib from the extended-release tablet. Indeed, the f2 similarity factor is 32.60 (< 50), indicating a low degree of similarity, signifying significant differences between the profiles.

In the case of USP Apparatus IV, the dissolution profile closely resembles that of the reference USP apparatus I with an f2 similarity factor of 69.64. After completion of the experiment, approximately 72% of upadacitinib was released across various media. Notably, despite using the same testing protocol for USP apparatus III and IV, the dissolution kinetics with USP apparatus IV appeared to be slower (Fig. 1C–D). This variance can be attributed to distinct hydrodynamics within the systems: the immersion and dipping action of the cylinder in water within USP Apparatus III may have had a more disruptive effect on the HPMC matrix compared to the fluid flow within the cells of USP Apparatus IV, which may better mimic the physiological motility conditions of the gastrointestinal tract.

The differences in the experimental protocols between the fed and fasted states primarily lie within the stomach compartment, involving variations in media composition, emptying time, and pH. In the fed state (FeSSGF), three phases (early, middle, and late) all include the oil-in-water emulsion Lipofundin to replicate the lipid content present in the stomach after ingestion of food. The tablet's residence time in the stomach was notably extended to 240 min in the fed state (FeSSGF) compared to the faster 60-min duration in the fasted state (FaSSGF). Furthermore, the pH level in the fed state was elevated to 5.0, in sharp contrast to the acidic pH of 1.6 in the fasted state.

In the dissolution experiments of RINVOQ® ER formulation conducted under fed state conditions, as illustrated in Fig. 2, we observed a narrower disparity in drug release between USP apparatus III and USP apparatus IV dissolution curves, as denoted by an f2 similarity factor of 53.36%.

Comparing these profiles to the USP apparatus I reference profile (A), USP apparatus IV (C) displayed a distinct pattern of drug release. It exhibited a reduction in drug release until the 420-min timepoint,

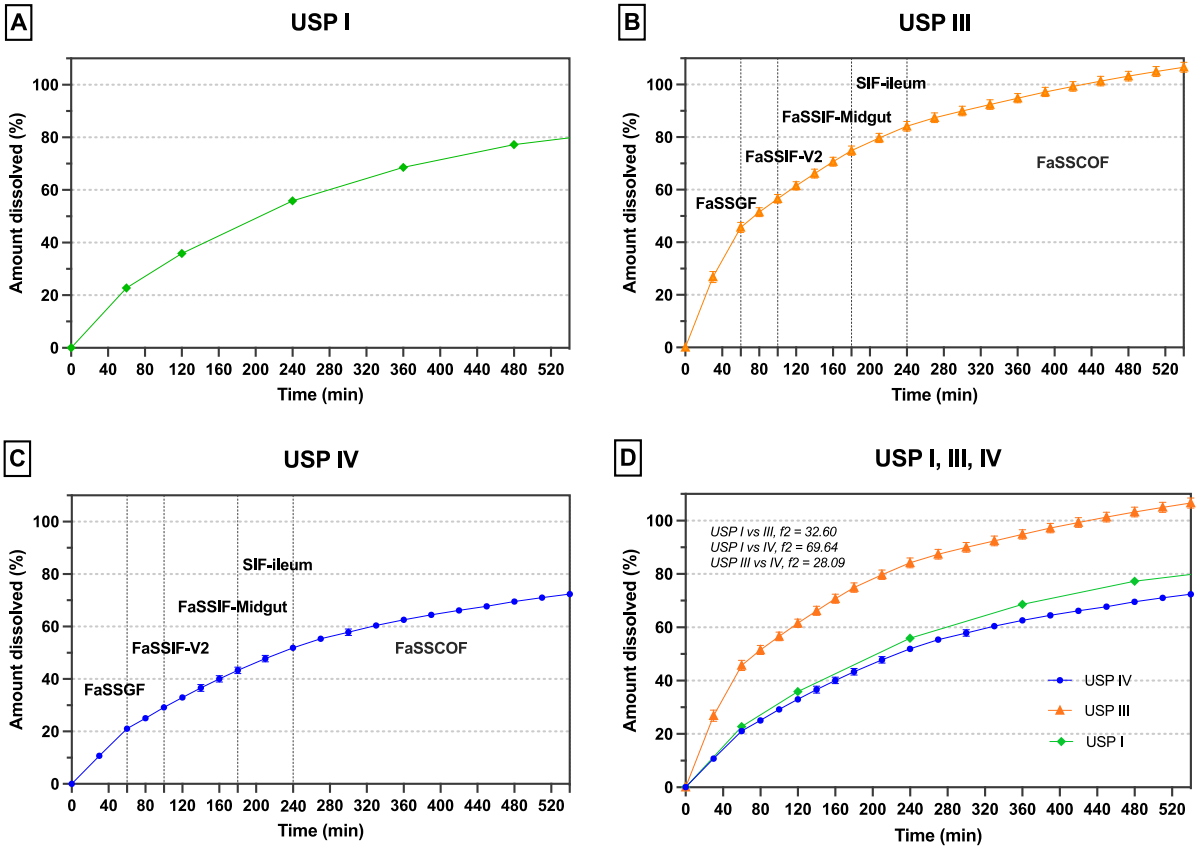

Fig. 1. A depicts the dissolution profile obtained using USP apparatus I, representing the reference method (adapted from Mohamed et al. [10]). B and C depict the dissolution profiles obtained using USP apparatus III and IV in the fasted state ($n = 6$ each), respectively. D presents a combined view of all three dissolution profiles for comparative analysis.

coinciding with the transition to FeSSCOF media, which is designed to mimic colonic fluid in the fed state. At this point, the drug release increased from 74.76% to reach a total of 88.11% by the end of the experiment. In contrast, USP Apparatus III (B) consistently showed slightly higher drug release throughout the entire experiment compared to both USP Apparatus I and IV, ultimately resulting in a total drug release of 89.67%.

3.2. Integration of USP dissolution profiles into PBPK modeling for plasma concentration predictions

PBPK methodologies have emerged as essential tools for forecasting the oral absorption of drugs, with the majority of applications focusing on IR drug products, whose absorption occurs mainly in the small intestine. Instead, the prediction of absorption of modified/extended-release formulations requires (i) model disposition parameters to be accurately defined, ideally through the availability of IV data but more usually through IR data, and (ii) *in vitro* biopredictive dissolution experiments to overcome the regional intestinal differences in absorption [22]. For instance, the majority of the models that integrate dissolution profiles of extended-release systems fit the data to an empirical function such as Weibull function. In Table 6, the Weibull function parameters, indicated as alpha and beta, for each USP apparatus used in this study were reported and these values were used accordingly to describe the dissolution in the GastroPlus™ software. As mentioned beforehand, no lag time was observed and a maximum release of 100% was shown throughout the dissolution experiments. This information was also integrated into the 1st order Weibull function.

3.2.1. Observed and predicted plasma concentration-time profiles

The initial objective of this study was to develop a robust PBPK model that would enable the comparison of observed PK to predicted values obtained through simulations that were driven by the different dissolution datasets generated through experimental studies. The model development used the human ADME data (Study M13–548 from the Clinical Pharmacology and Biopharmaceutics Review(s) [10]), based on a 30 mg oral solution of upadacitinib administered to 4 healthy subjects, and the 24 mg immediate-release formulation (from Mohamed et al. [10]) for the systemic pharmacokinetic parameters. Model validation, on the other hand, was conducted using data from three additional clinical studies (Table 4). Studies M15–878 and M14–680 allowed for the evaluation of the food effect on upadacitinib plasma concentrations (Table 4). The novelty of this project lies in examining the plasma concentration predictions resulting from the adoption of different Weibull functions derived from distinct dissolution profiles, demonstrating the crucial interplay between dissolution kinetics and predictive modeling.

In the study conducted by Mohamed and co-workers [10], a cohort of 20 healthy subjects, under fasting conditions, was enlisted for the administration of a prototype formulation of the planned commercial formulation, and their plasma concentration values were used for model verification. With the term 'model verification', we refer to the predicted *versus* observed ratios for plasma C_{max} and AUC for a range of clinical studies to see how our model is able to predict systemic exposure within a certain prediction error. In the graphs shown in Fig. 3, the red dots represent the observed data, while the blue continuous line represents the corresponding predictions generated by the PBPK model. The *in vivo* data revealed a median plasma C_{max} value of 59.5 ng/mL and a median plasma T_{max} value of 3.0 h (Table 7). To assess the performance of our

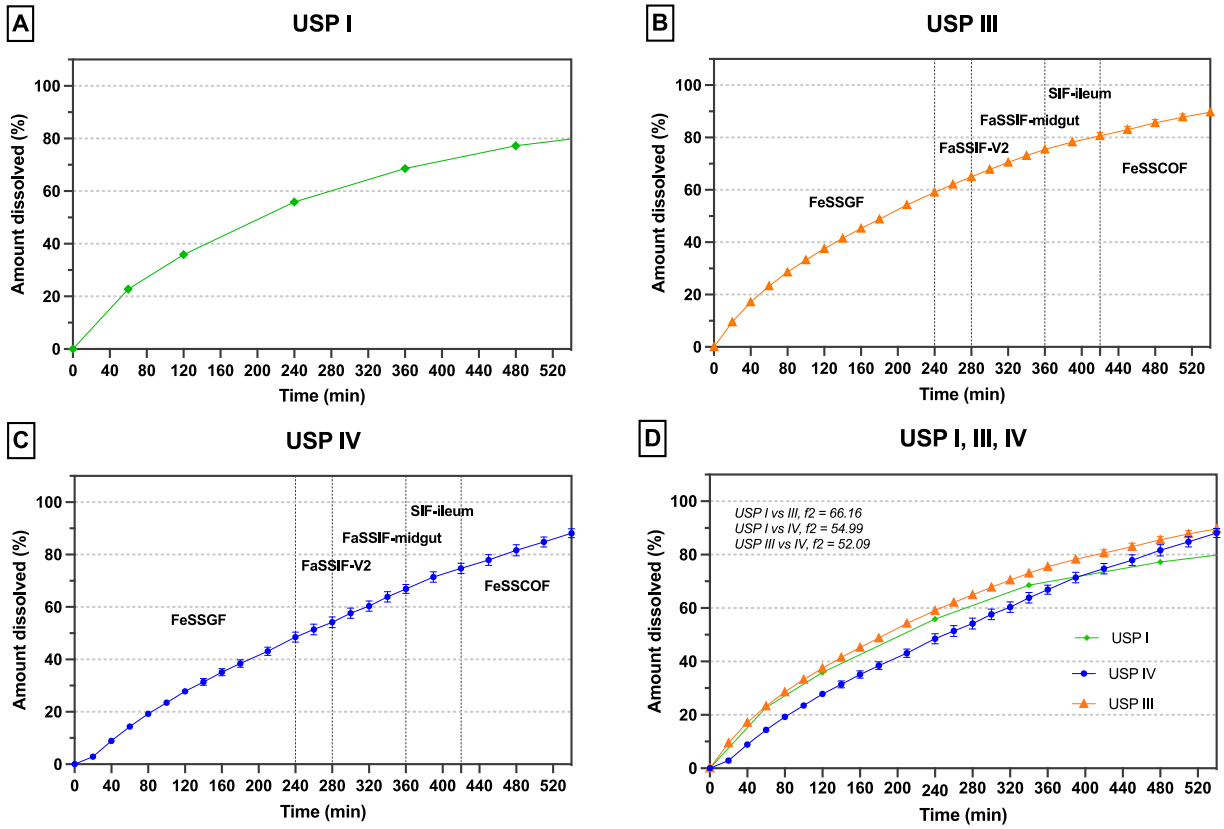

Fig. 2. A depicts the dissolution profile obtained using USP apparatus I, representing the reference method (adapted from Mohamed et al. [10]). B and C depict the dissolution profiles obtained using USP apparatus III and IV in the fed state ($n = 6$ each), respectively. D presents a combined view of all three dissolution profiles for comparative analysis.

Table 6
Weibull function parameters for different USP dissolution profiles, assuming Fmax = 100% and lag time = 0.

Weibull function parameters		
USP I (Formulation C)	Alpha	3.7409
	Beta	0.80065
USP III - fasted	Alpha	1.8953
	Beta	0.93798
USP IV - fasted	Alpha	4.2381
	Beta	0.78876
USP III - fed	Alpha	4.1953
	Beta	0.98249
USP IV - fed	Alpha	7.6163
	Beta	1.2009

PBPK model under varying dissolution profiles as inputs, we employed 1st order Weibull functions derived from USP apparatus I, III, and IV.

Notably, when employing the Weibull functions from USP apparatus I and IV, our PBPK model yielded precise predictions for *in vivo* plasma concentrations, consistently falling within limits ranging from 0.5 to 1.5 when comparing predicted parameters (including plasma C_{max}, T_{max}, and AUC) with observed values (Table 7). Conversely, the overestimation of upadacitinib dissolution observed in the USP apparatus III dissolution experiment manifested in our PBPK predictions as well. Specifically, the plasma C_{max} calculated by the PBPK model reached 79.8 ng/mL, surpassing the observed clinical study value of 59.5 ng/mL. This confirms the model's sensitivity to the choice of dissolution profiles through Weibull functions. Studies M15–878 and M14–680 enrolled 42 and 12 healthy subjects, respectively, under both fasted and fed conditions.

In the case of studies M15–878 and M14–680 conducted under fed state conditions, Weibull functions from both USP III and USP IV dissolution profiles were employed. The predictions showed similar results, irrespective of whether USP III or USP IV profiles were employed, as supported by the dissolution data showing an f2 similarity factor of 53.36 between the two experiments. However, when scrutinizing these predictions in light of the observed *in vivo* data, a common trend emerged; none of the two dissolution profiles managed to precisely replicate the actual *in vivo* drug release dynamics: the prediction curve showed a quicker absorption of the active drug in the plasma, represented by the alteration in plasma T_{max}, and reduced C_{max} in all cases. This finding suggests that the fed state protocol employed for the dissolution experiments may not reflect the complexities of *in vivo* drug behavior in a fed state scenario. Indeed, the composition of a meal, with fats, proteins, and carbohydrates, can interact with the drug, modulate gastric emptying, and induce dynamic pH changes, collectively affecting drug dissolution and absorption. Further investigations into the physiological intricacies of the fed state may be necessary to refine the drug release mechanisms, to then improve *in vitro* dissolution tests to accurately replicate these conditions.

3.3. IVIVC

In order to evaluate the biopredictive abilities of the different dissolution methods tested (USP I, USP III, and USP IV), an attempt to develop a Level A IVIVC was made. *In vivo* data for the plasma concentration of upadacitinib 30 mg ER formulation, deconvoluted to fraction absorbed (Fa) was found in the manuscript published by Mohamed et al. [10]. The *in vivo* data were then plotted against the *in vitro* data obtained in the present study, indicated as 'the fraction dissolved *in vitro*'. It is important mentioning that the *in vivo* data were collected in fasted state subjects, therefore, the correlation was

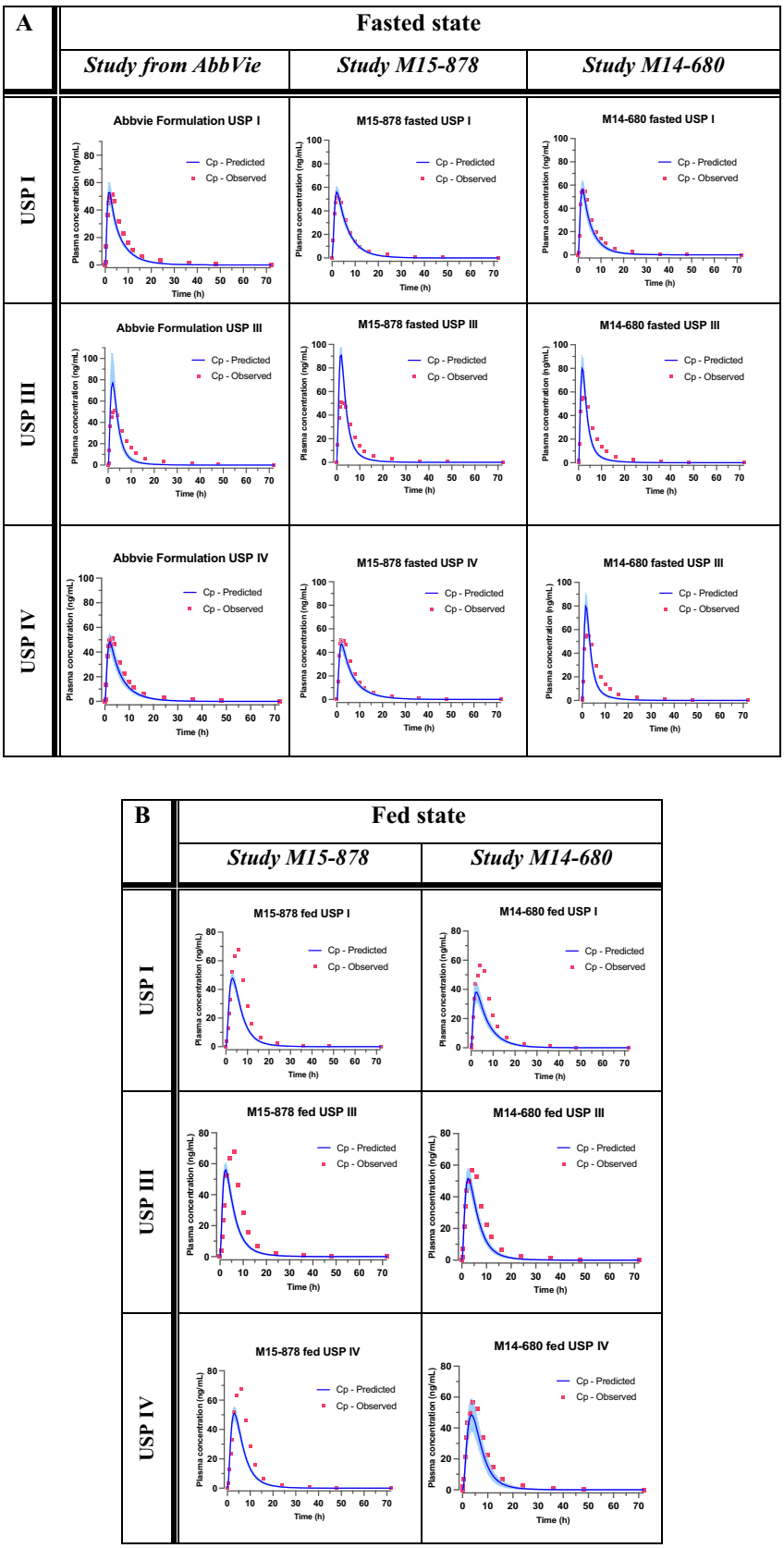

Fig. 3. Observed and predicted mean plasma concentrations -time profiles for upadacitinib after oral administration of a solution (Study M13–548 [17]), and an extended-release formulation (study from Mohamed et al. [10]). In each graph, the blue line represents the predicted plasma concentration in 72 h, the red dots represent the relative plasma concentration observed *in vivo* in the respective studies, and the blue shade corresponds to the 90% confidence upper and lower limit of the predictions. Fig. 3 A depicts the predicted plasma concentrations in fasted state, B depicts the predicted plasma concentrations in fed state. (For interpretation of the references to colour in this figure legend, the reader is referred to the web version of this article.)

Table 7
PBPK model-predicted and observed (mean ± % CV or range) upadacitinib exposures based on input of different dissolution profiles to describe the absorption of upadacitinib. Abbreviations: AUC_{inf}, area under the concentration-time curve from time zero to infinity; C_{max}, observed maximum concentration; obs, observed; pred, predicted; SD, standard deviation; T_{max}, time of observed maximum concentration. IR, immediate release tablet, ER, extended-release tablet. (a) Median.

Study	Upadacitinib formulation	Dissolution input data	Predicted/Observed			
			C_{max} (ng/mL)	T_{max} (h)	AUC_t (ng hr/mL)	AUC_∞ (ng hr/mL)
M13–548 (ADME), (n = 4)	Oral solution, 30 mg	Johnson-Noyes dissolution model	1.03	1.13	0.81	0.81
AbbVie [23] (n = 20)	Immediate Release capsule, 24 mg	Johnson-Noyes dissolution model	0.88	0.98	0.71	0.71
AbbVie [23] (n = 20)	ER, 30 mg, formulation A, 10% HPMC, fasted state	USP I	0.95	1.06	0.73	0.71
AbbVie [23] (n = 20)	ER, 30 mg, formulation B, 15% HPMC, fasted state	USP I	1.01	0.88	0.85	0.83
AbbVie [23] (n = 20)	ER, 30 mg, formulation C 20% HPMC, fasted state	USP I	0.94	0.64	0.70	0,69
AbbVie [23] (n = 20)	ER, 30 mg, formulation D, 30% HPMC, fasted state	USP I	0.89	0.78	0.77	0.73
AbbVie [23] (n = 20)	ER, 30 mg, formulation C, 20% HPMC, fasted state	USP III, fasted	1.56	0.61	0.80	0.79
AbbVie [23] (n = 20)	ER, 30 mg, formulation C, 20% HPMC, fasted state	USP IV, fasted	0.85	0.67	0.69	0.68
M15–878 (n = 42)	ER18, 30 mg, fasted state	USP I	1.02	1.1	0.83	0.81
M15–878 (n = 42)	ER18, 30 mg, fasted state	USP III, fasted	1.63	0.9	0.85	0.83
M15–878 (n = 42)	ER18, 30 mg, fasted state	USP IV, fasted	0.84	1.05	0.73	0.71
M14–680 (n = 12)	ER8, 30 mg, fasted state	USP I	0.91	0.9	0.70	0.68
M14–680 (n = 12)	ER8. 30 mg, fasted state	USP III, fasted	1.29	0.85	0.69	0.67
M14–680 (n = 12)	ER8. 30 mg, fasted state	USP IV, fasted	0.75	1.15	0.74	0.72
M14–680 (n = 12)	ER8, 30 mg, fed state [2]	USP I	0.52	0.68	0.55	0.54
M14–680 (n = 12)	ER8, 30 mg, fed state [2]	USP III, fed	0.69	0.68	0.64	0.63
M14–680 (n = 12)	ER8, 30 mg, fed state [2]	USP IV, fed	0.64	0.9	0.64	0.65
M15–878 (n = 42)	ER18, 30 mg, fed state [1]	USP I	0.61	0.5	0.58	0.57
M15–878 (n = 42)	ER18, 30 mg, fed state [1]	USP III, fed	0.74	0.4	0.60	0.59
M15–878 (n = 42)	ER18, 30 mg, fed state [1]	USP IV, fed	0.66	0.5	0.61	0.60

calculated between the dissolution profiles of RINVOQ® in biorelevant media mimicking the fasted state exclusively.

The correlation plots obtained are presented in Fig. 4. USP I represents the dissolution method published by AbbVie Inc. [10], which exhibited a strong correlation with the *in vivo* data, featuring a coefficient of determination (R^2) of 0.9839 and a slope value of 0.8373. While these values are close to unity, suggesting a robust linear relationship between the independent and dependent variables in the regression model, an even stronger correlation was observed between the fraction absorbed *in vivo* and the fraction dissolved in the USP IV apparatus. This correlation yielded a slope value of 0.9262 and an R^2 of 0.9875, aligning closely with the results from USP I. Moreover, the % prediction error (% PE) for USP IV was −2.67%, resulting in the establishment of a Level A IVIVC, as in agreement with FDA Guidance for Industry: Extended Release Oral Dosage Forms: Development, Evaluation, and Application of *In Vitro/In Vivo* Correlations [19]. In contrast, USP III, which overestimated *in vitro* drug release and consequently resulted in inaccurate drug plasma concentration-time predictions in GastroPlus™, was still close to the establishment of Level A IVIVC, with a slope value of 0.6348 and an R^2 of 0.9632 with a −10.1% Mean PE value.

3.4. Extrapolation of the colonic luminal concentration/absorption

The PBPK model developed for both fasted and two fed state

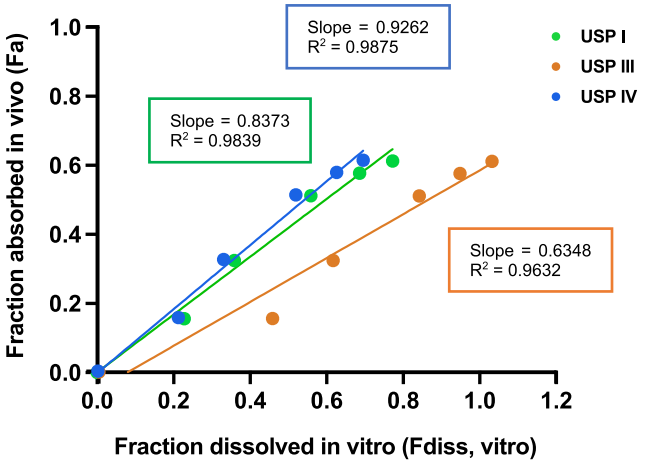

Timepoints (h)	Fraction absorbed	%PE		
		USP I	USP III	USP IV
0	0	0	0	0
1	0.15559	-22.6	-55.1	-23.1
2	0.32415	7.29	-5.56	7.07
4	0.51216	8.62	5.15	6.89
6	0.57699	0.37	4.04	0.22
8	0.61264	-5.61	0.94	-4.48
Mean %PE		-2.39	-10.1	-2.67
Std Dev		12.7	25.5	12.4

Fig. 4. IVIVC correlation between Fa *in vivo*, and Fdiss *in vitro* (specifically, USP I, III, and IV), in fasted state, with corresponding %prediction errors (PE) calculated for each timepoint, and mean %PE.

conditions allowed us to extract the colonic concentrations of upadacitinib as predicted by the model. We simulated different drug concentrations (2, 5, 15, 30, and 45 mg) in each of these scenarios and calculated both the maximum luminal and enterocyte concentrations in the ascending colon GI compartment for each simulation. The resulting values were then plotted against the corresponding plasma $AUC_{0\text{-}t}$ and C_{max} to explore the correlation between the systemic concentration of upadacitinib and its local concentration in the colon (Fig. 5).

The observed correlations demonstrated a perfect linear relationship with a coefficient of determination (R^2) equal to 1 or close to 1. This indicates that as the colonic concentration of the drug changes, the associated $AUC_{(0\text{-}t)}$ and C_{max} values change proportionally. Such a finding suggests a highly predictable and consistent relationship between the colonic drug concentration and key pharmacokinetic parameters, underscoring that alterations in colonic drug levels have a direct, uniform impact on the drug's overall absorption (*i.e.,* rate and extent) throughout the body.

Nevertheless, it's worth noting that a direct correlation isn't always applicable, as exemplified by the case of celecoxib. In this instance, caecal tissue concentrations of the drug and its metabolite were substantially higher despite a decrease in plasma concentrations [24]. The accumulation of a substantial solid fraction of celecoxib in the cecum is attributed to its low solubility in the small intestine and suboptimal dissolution conditions in the colonic lumen, characterized by low fluid volumes and increased viscosity [24].

3.5. Strengths and limitations of the PBPK model in the integration of different dissolution profiles

The incorporation of *in vitro* dissolution data into a PBPK model can be approached in various ways, depending on the drug's specific characteristics and formulation [22]. Upadacitinib, characterized by its high permeability and solubility, can be considered as a BCS Class I drug [25], indicating complete dissolution in the intestinal environment and a reduced susceptibility to physiological variations and inter-subject differences. Typically, dissolution profiles of BCS Class I drugs are directly integrated into the PBPK model or dissolution can be described as a function of the residual GI pH in combination with Noyes-Whitney equation to describe dissolution as a function of particle size and solubility (indicating the maximum extent of dissolved drug) [26]. However, the formulation of upadacitinib as an extended-release product, employing hypromellose (Methocel K4M) as a major excipient to form a matrix tablet [27], necessitated the use of an empirical Weibull function for the integration of dissolution data as previously suggested in other studies [28,29].

The time scale parameter (alpha) and shape parameter (beta) of the Weibull function offer the capability to describe a wide range of dissolution profiles, including those from USP apparatus I, III, and IV in this

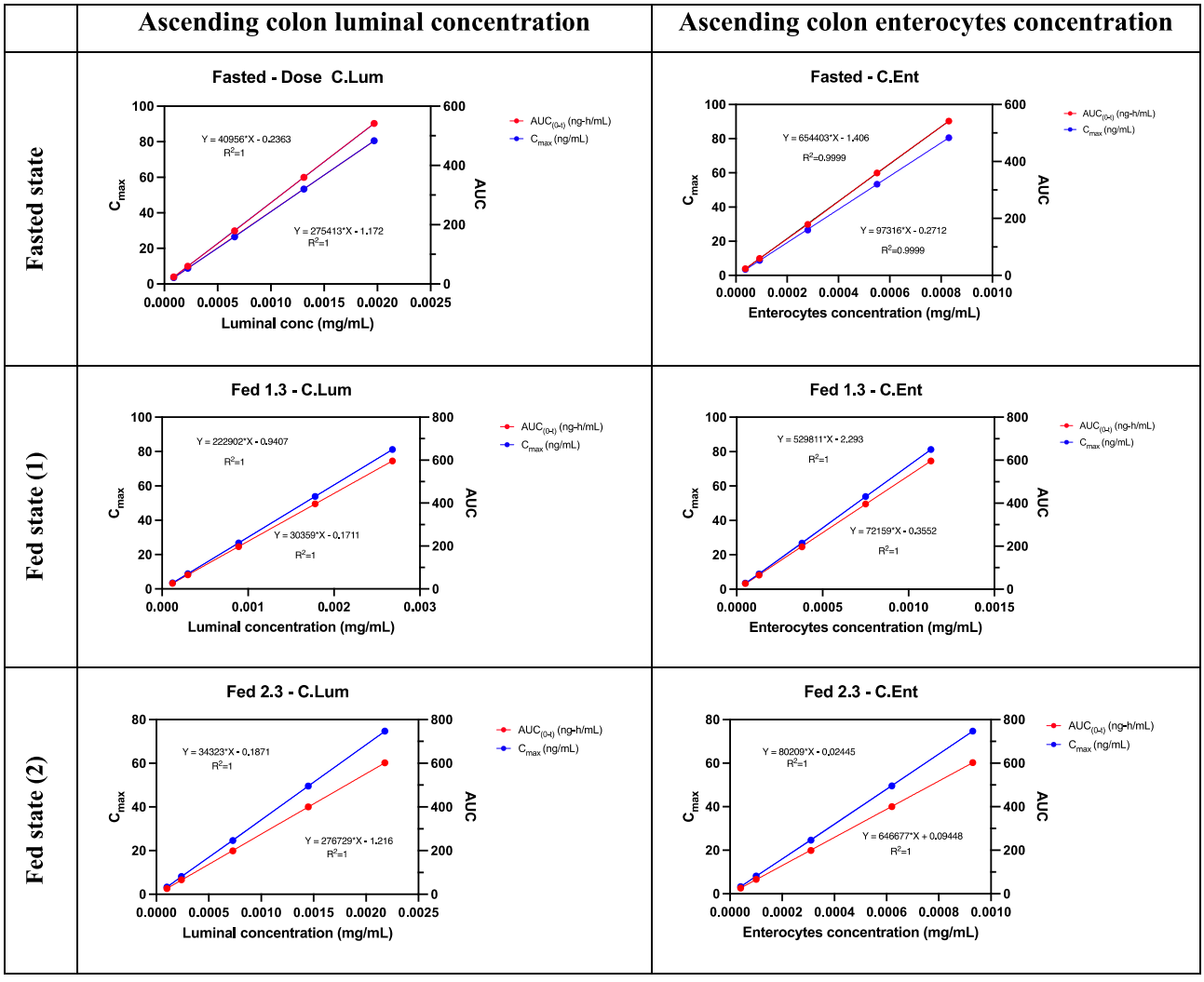

Fig. 5. Correlation analysis of drug concentration in both luminal and enterocytes of the ascending colon, with systemic pharmacokinetic parameters (plasma $AUC_{0\text{-}t}$ and C_{max}). Fed state (1) has a stomach transit time of 1h30min, Fed state (2) has a stomach transit time of 2h30min.

study. Notably, our PBPK model exhibited significant sensitivity to variations in the input dissolution profiles. Modifying the Weibull functions (alpha and beta parameters, assuming F_{max} = 100% and lag time = 0) for different dissolution experiments resulted in substantial alterations in the model's predictions.

The model sensitivity became evident when using the USP III apparatus with biorelevant media simulating the fasted state (as illustrated in Fig. 1), which demonstrated complete drug release (107%) within a 9-h experiment. Integrating the Weibull function from this specific dissolution profile into the PBPK model resulted in a noticeable overestimation of both plasma C_{max} and T_{max}. Indeed, compared to USP IV which showed a Level A IVIVC correlation and accurately depicted the drug's release behavior from its formulation, for USP III, the ratio of predicted/observed exposures was closer to the boundary limit of 1.5. C_{max} for the three studies (AbbVie study, M15–878, and M14–680) included in the model validation, and were respectively 1.56, 1.63, and 1.29 (Table 7 and Fig. 3). The corresponding plasma C_{max} values for the same studies when the USP IV dissolution profile was integrated, were 0.85, 0.84, 0.75 (Table 7 and Fig. 3), closer to the optimal value of 1. This capability holds significant potential for optimizing various formulations of the same drug. For instance, in the case of extended-release formulations with differing percentages of hypromellose (HPMC), the integration of distinct dissolution profiles into the model can supply crucial insights into how changes in formulation impact *in vivo* drug release kinetics. Consequently, this information can play a pivotal role in shaping decisions related to formulation design and dosing regimens during the drug development process.

However, the model's sensitivity holds also significant limitations. Specifically, the model's inability to distinguish between various dissolution media, account for varying pH levels, or consider the different durations the formulation spends in each medium can affect its accuracy in predicting the *in vivo* behavior of pharmaceutical formulations. This discrepancy becomes especially evident when the drug's behavior is sensitive to pH variations, as seen when using media with different pH and compositions. Indeed, the Weibull function, used as a dissolution input, cannot effectively account for bile salts and pH-dependent variations in different GI compartments. Therefore, testing the drug product in presence of biorelevant media needs to be considered prior to using this dissolution function in GastroPlus™. In addition, the applied *in vitro* models do not simulate the strong contractions of the stomach that might affect formulation performance. For example, strong bursts of phase 2/3 contractions might release more amount of the drug when passing through the pylorus from the stomach to the small intestine [30]. Nevertheless, when integrating the observed dissolution profiles to reflect the *in vivo* dissolution rate in the modeling software, good matches were observed when comparing the absorption phase of the simulations *versus* the absorption phase of the observed systemic exposure data. This could suggest that the strong burst of gastric contractions might not be so effective towards formulation rupture or extensive erosion of the matrix tablet.

3.6. Evaluating HPMC matrix behavior in USP III and IV apparatus

Hydroxypropyl methylcellulose (HPMC) is a water-swellable hydrophilic matrix [31], frequently employed in controlled-release dosage forms. As it transits throughout the GI tract, HPMC swells, allowing water to penetrate the dosage form. Concurrently, disentangled polymers on the surface erode, facilitating the diffusion of the drug from the solid core. This process, involving both drug diffusion and erosion, typically occurs simultaneously, especially for highly soluble drugs like upadacitinib [31].

Selecting the appropriate *in vitro* dissolution technique for modified release formulation is challenging. The choice of the USP Apparatus is not standardized and needs to take into consideration the properties of the ER system, whether it be a matrix system, microspheres, an osmotic pump, or a layered tablet, in addition to the characteristics of the other excipients and API [32]. Traditionally, the use of USP I is discouraged for hydrophilic matrix (*e.g.,* HPMC), because of their swelling, which may result in clogging of the holes in the basket disrupting the hydrodynamics of the experiment.

In this study, our objective was to assess the clinical relevance of USP apparatus III and IV under both fasted and fed states. Apparatus III is suited for extended-release (ER) formulations due to its ability to transition the cylinders from one media to the next, thereby introducing the dosage form into a cumulatively larger volume of media over the time course of the dissolution test, surpassing the 1 L limit of apparatus I and II. This technology has been employed in several studies to evaluate drug release from HPMC-based formulations [33–35] under various GI prandial conditions. Among the three dissolution apparatuses investigated in this study, however, USP III exhibited the lowest suitability for predicting *in vivo* data (R^2 = 0.9632, Fig. 4). The experimental protocol employed for USP III was identical to that used for USP IV. Therefore, the discrepancy in drug release must have arisen from the mechanical action of the basket in USP III, which may have contributed to matrix disruption and potentially accelerated drug release. This phenomenon was especially evident during the first hour of the experiment in FaSSGF media at pH 1.2, where the hydrodynamics within the vessel, combined with the media's acidic nature favoring higher solubility of the active compound, likely led to the dissolution of approximately 50% of the drug in the media.

In contrast, USP IV, known for providing more controlled and consistent flow conditions, resulted in roughly 20% of the drug being dissolved within the initial hour of the experiment, resulting in a successful Level A IVIVC (R^2 = 0.9875, Fig. 4). The drug's release from FaSSIF to FaSSCOF media had similar profiles for both USP III and IV. However, the dip rate used in the USP III protocol (12 in FaSSGF-10 in FaSSIF-SIF ileum-6 in FaSSCOF) was comparable to what has been previously employed for experiments assessing drug release from HPMC tablets under fasted conditions [33–35].

The fed state media demonstrated a decreased release rate of upadacitinib from the extended-release (ER) tablet compared to fasted state conditions. Specifically, in USP III, the reduction in drug release amounted to 16.3% compared to the fasted state, while in USP IV, the fed media initially caused a reduction in drug release until 300 min, after which a positive effect was observed until the end of the experiment. Overall, drug release in both systems was comparable, with 88.11% released in USP IV and 89.67% in USP III, respectively. Notably, the FeSSGF media maintained a pH of 5.0 in the early, middle, and late phases (0 to 240 min) of the run, with this pH being responsible for 60% drug release in USP III and 50% in USP IV within 4 h of the experiment. This observation can be attributed to a decreased availability of water for upadacitinib dissolution and diffusion in and out of the HPMC matrix. The diminished rate of water permeation into the matrix results in reduced polymer relaxation and tablet erosion. Moreover, it is important to specify that FeSSGF is made of Lipofundin emulsion, with 20% of fat content. Williams et al. [36] in their study showed that lipids in the media may interact with the HPMC tablet forming a hydrophobic barrier that hinders the rate of fluid penetration into the tablet. Specifically, they observed a retarded drug release in the presence of high-fat emulsions: fat deposed in the outer surface of the gel layer, both in the early stages of gel layer formation and up to 8 h as noted in the USP IV apparatus.

However, the *in vivo* scenario may differ significantly from the *in vitro* situation due to the vigorous mixing in the stomach and the presence of gastric and pancreatic lipases, which can transform fat deposits into more soluble forms, making them ready for absorption. These intrinsic processes may limit or even prevent the formation of fat deposits on tablet surfaces. This could explain the disparity in the food effect observed in this study when comparing *in vitro* and *in vivo* data: food increased plasma C_{max} by 39% and $AUC_{0\text{-inf}}$ by 29% in the clinical study M15–878, and it increased plasma C_{max} by 18% and $AUC_{0\text{-inf}}$ by 30% in the clinical study M16–094. It becomes evident that *in vivo* digestive

processes, including the transformation of fat deposits by gastric and pancreatic lipases, and the presence of digested materials are not adequately captured in conventional *in vitro* setups with the risk that the dosage form may physically interact with the fat component of the medium, causing altered drug release patterns. This limitation underscores the need for caution when using fat emulsions as components in 'biorelevant' dissolution test media to predict *in vivo* effects on HPMC matrix systems.

3.7. Biorelevant media does not always imply biopredictive dissolution testing

Dissolution media are categorized into four levels of luminal composition simulation. Level 0 media consists of simple aqueous solutions with pH adjusted to represent the pH in the specific section of the GI tract. In Level I media, both pH and buffer capacity are adjusted to reflect physiological values. Additionally, bile components, dietary lipids, and key digestion products are included in Level II media to mimic the solubilization capacity of luminal fluids, addressing differences in luminal composition between the fasted and fed states, as used in our study. Level III media, the most complex compositions, also consider proteins, enzymes typically present in the aqueous phase of luminal contents, and viscosity effects on drug release [18,37].

While biorelevant media, designed to mimic the GI fluids, have the potential to improve the physiological relevance of *in vitro* drug release testing, it is not necessarily always the case that their use always delivers results that are biopredictive. Interestingly, the present work results challenge the conventional perception that this is the case. For example, the use of USP I experimental conditions, characterized by a phosphate buffer rather than biorelevant media, demonstrated a Level A IVIVC (R^2 = 0.9839, Fig. 4). In contrast, experiments conducted using USP III with biorelevant media, designed to faithfully replicate the physiological environment, did not yield Level A biopredictive outcomes (Fig. 4). This disparity underscores the complexity of drug release mechanisms and suggests that biorelevant media may not universally guarantee superior biopredictive accuracy. For instance, upadacitinib demonstrates a high solubility at pH values around 2–3 (10.5 mg/mL) and 9 (0.199 mg/mL) as shown in Table 5. The characteristics of the drug may be responsible for the fact that the drug showed similar release profiles, with good *in vivo* correlation, for both USP I and USP IV despite the use of biorelevant media or a phosphate buffer. Still, differences in dissolution model setup may result in distinct dissolution profiles among different setups (*e.g.*, USP I/IV *versus* USP III). For poorly soluble drugs, however, the impact of biorelevant media on drug release will be more pronounced. Fluctuations in the pH and bile salt/ phospholipid levels as reproduced by the different biorelevant media can be essential to accurately mimic the *in vivo* situation. Especially for lipophilic compounds, which may encounter challenges related to wetting, the presence of physiological levels of bile salts can facilitate wetting, potentially leading to drug solubilization and addressing solubility issues commonly encountered in basic buffer solutions [38].

3.8. The colonic concentration of the drug

We mentioned how the Medicine Agencies (EMA and FDA) suggest a bioavailability assessment of drugs in the colon through the measurement of systemic plasma drug concentration instead of correctly measuring the drug available at the site of action. With the help of PBPK predictions, it was possible to estimate the concentration (and amount in mg) of upadacitinib that reaches the ascending colon of a person in both fasted and fed conditions. Based on the simulations in Fig. 5, a positive, linear regression was observed between plasma C_{max} and $AUC_{(0\text{-}t)}$ *versus* colonic concentrations (*i.e.,* luminal and intracellular). Thus, results indicate that the drug's concentration in the colon directly affects its absorption into the bloodstream, making it a crucial factor in determining the drug's pharmacokinetics and its subsequent therapeutic effects.

However, although predicted plasma concentrations were in line with the observed plasma concentrations, cautiousness should be considered as we assume instantaneous distribution/equilibrium in the model. We should further explore this when performing *in vivo* studies (*i.e.*, taking biopsies from colonic tissue and extracting the intracellular concentration of the tissue, as studied by Lemmens et al. for celecoxib and sulindac [24,39]) or exploring the equilibrium constant rate in an *in vitro* set up (*e.g.,* adding relevant luminal concentrations of the drug at the apical side of the Caco-2 cell monolayer and studying the accumulated drug as a function of time).

Knowing the colonic concentration has the advantage of more accurate predictive models, aiding in the design and interpretation of *in vitro* experiments. Researchers can better mimic *in vivo* conditions by incorporating relevant drug concentrations, which can lead to more realistic and informative results.

Understanding colonic concentration in both lumen and enterocytes not only enhances the relevance, predictive power, and cost-effectiveness of *in vitro* techniques but also holds particular significance for pharmacokinetic/pharmacodynamic considerations for the development of locally acting drugs. Based on this approach, relevant drug concentrations can be applied to study drug *versus* microbiota interactions in *in vitro* colonic disposition models.

4. Conclusion

The increasing utilization of extended-release formulations brings with it a need to comprehend and quantify how these formulations release drugs along the GI tract establishing a link with PK/PD profiles. Our study introduces a novel IVIVC protocol that evaluates the predictive accuracy of different USP dissolution apparatuses against *in vivo* corresponding data. Specifically, USP IV demonstrated a Level A IVIVC for RINVOQ® hypromellose extended-release formulation, suggesting how this apparatus could potentially be the most precise in mimicking the GI conditions for HPMC-based MR formulations. Moreover, the integration of biopredictive dissolution testing with PBPK modeling allowed for a deeper understanding of upadacitinib absorption in the GI tract, especially in the colon. This is particularly important for drugs that are active in the large intestine and for *in vitro* studies looking at how specific drug concentrations affect the microbiota and *vice versa*.

CRediT authorship contribution statement

Alessia Favaron: Writing – original draft, Visualization, Formal analysis, Data curation, Conceptualization. **Bart Hens:** Writing – review & editing, Supervision, Software. **Maiara Camotti Montanha:** Writing – review & editing, Methodology, Investigation. **Mark McAllister:** Supervision, Resources, Project administration. **Irena Tomaszewska:** Investigation, Methodology. **Shaimaa Moustafa:** Investigation. **Marília Alvarenga de Oliveira:** Formal analysis. **Abdul W. Basit:** Supervision. **Mine Orlu:** Funding acquisition, Supervision.

Data availability

Data will be made available on request.

Acknowledgments

This work was supported by the European Union's Horizon 2020 research and innovation program COLOTAN under the Marie Skłodowska-Curie grant agreement no. 956851. Authors have no (financial) conflicts of interest to declare.

Appendix A. Supplementary data

Supplementary data to this article can be found online at https://doi.

org/10.1016/j.jconrel.2024.04.024.

References

[1] EMA. European Medicines Agency, [Cited 2023 Jul 28]. Rinvoq, Available from: https://www.ema.europa.eu/en/medicines/human/EPAR/rinvoq, 2019.

[2] N. Kavanagh, O.I. Corrigan, Swelling and erosion properties of hydroxypropylmethylcellulose (hypromellose) matrices–influence of agitation rate and dissolution medium composition, Int. J. Pharm. 279 (1–2) (2004 Jul 26) 141–152.

[3] G. Gujral, D. Kapoor, M. Jaimini, An updated review on modified release tablets, J. Drug Deliv. Therap. 8 (4) (2018 Jul 14) 5–9.

[4] EMA, Guideline on the pharmacokinetic and clinical evaluation of modified release dosage forms [cited 2023 Sep 5]; Available from: https://www.ema.europa.eu/en/documents/scientific-guideline/guideline-pharmacokinetic-and-clinical-evaluation-modified-release-dosage-forms_en.pdf.

[5] M.A. García, F. Varum, J. Al-Gousous, M. Hofmann, S. Page, P. Langguth, In vitro methodologies for evaluating Colon-targeted pharmaceutical products and industry perspectives for their applications, Pharmaceutics 14 (2) (2022 Jan 26) 291.

[6] EMA, Guideline on the investigation of bioequivalence [Internet] [cited 2024 Feb 7]. Available from: https://www.ema.europa.eu/en/documents/scientific-guideline/guideline-investigation-bioequivalence-rev1_en.pdf.

[7] C.J. Andreas, Y.C. Chen, C. Markopoulos, C. Reppas, J. Dressman, In vitro biorelevant models for evaluating modified release mesalamine products to forecast the effect of formulation and meal intake on drug release, Eur. J. Pharm. Biopharm. 97 (2015 Nov) 39–50.

[8] C. Reppas, N.N. Vrettos, J. Dressman, C.J. Andreas, Y. Miyaji, J. Brown, et al., Dissolution testing of modified release products with biorelevant media: an OrBiTo ring study using the USP apparatus III and IV, Eur. J. Pharm. Biopharm. 156 (2020 Nov 1) 40–49.

[9] K. Asare-Addo, B.R. Conway, H. Larhrib, M. Levina, A.R. Rajabi-Siahboomi, J. Tetteh, et al., The effect of pH and ionic strength of dissolution media on in-vitro release of two model drugs of different solubilities from HPMC matrices, Colloids Surf. B Biointerfaces 111 (2013 Nov 1) 384–391.

[10] M.E.F. Mohamed, S. Trueman, A.A. Othman, J.H. Han, T.R. Ju, P. Marroum, Development of in vitro–in vivo correlation for upadacitinib extended-release tablet formulation, AAPS J. 21 (6) (2019 Oct 25) 108.

[11] J. Mann, J. Dressman, K. Rosenblatt, L. Ashworth, U. Muenster, K. Frank, et al., Validation of dissolution testing with biorelevant media: an OrBiTo study, Mol. Pharm. 14 (12) (2017 Dec 4) 4192–4201.

[12] C.J. Andreas, Y.C. Chen, C. Markopoulos, C. Reppas, J. Dressman, In vitro biorelevant models for evaluating modified release mesalamine products to forecast the effect of formulation and meal intake on drug release, Eur. J. Pharm. Biopharm. 97 (2015 Nov) 39–50.

[13] D. Mukherjee, M.S. Chiney, X. Shao, T.R. Ju, M. Shebley, P. Marroum, Physiologically based pharmacokinetic modeling and simulations to inform dissolution specifications and clinical relevance of release rates on elagolix exposure, Biopharm. Drug Dispos. 43 (3) (2022 Jun) 98–107.

[14] X. Li, Y. Yang, Y. Zhang, C. Wu, Q. Jiang, W. Wang, et al., Justification of biowaiver and dissolution rate specifications for piroxicam immediate release products based on physiologically based pharmacokinetic modeling: an in-depth analysis, Mol. Pharm. 16 (9) (2019 Sep 3) 3780–3790.

[15] R.L.M. Paraiso, R.H. Rose, N. Fotaki, M. McAllister, J.B. Dressman, The use of PBPK/PD to establish clinically relevant dissolution specifications for zolpidem immediate release tablets, Eur. J. Pharmaceut. Sci. Off. J. Eur. Feder. Pharmaceut. Sci. (2020 Dec 1) 155.

[16] C. Wagner, K. Thelen, S. Willmann, A. Selen, J.B. Dressman, Utilizing in vitro and PBPK tools to link ADME characteristics to plasma profiles: case example nifedipine immediate release formulation, J. Pharmaceut. Sci. [Internet]. 102 (9) (2013 Sep) [cited 2023 Sep 12]. Available from: https://pubmed.ncbi.nlm.nih.gov/23696038/.

[17] FDA, Clinical Pharmacology and Biopharmaceutics Review (RINVOQ), Center for Drug Evaluation and Research [Internet] [cited 2023 Aug 8]. Available from: https://www.accessdata.fda.gov/drugsatfda_docs/nda/2019/211675Orig1s000ClinPharmR.pdf.

[18] C. Reppas, N.N. Vrettos, J. Dressman, C.J. Andreas, Y. Miyaji, J. Brown, et al., Dissolution testing of modified release products with biorelevant media: an OrBiTo ring study using the USP apparatus III and IV, Eur. J. Pharm. Biopharm. 156 (2020 Nov 1) 40–49.

[19] FDA, Guidance for industry, dissolution testing of immediate release solid oral dosage forms [Internet]. [cited 2024 Feb 7]. Available from: https://www.fda.gov/media/70936/download, 1997.

[20] B. Hens, M.B. Bolger, Application of a dynamic fluid and pH model to simulate intraluminal and systemic concentrations of a weak base in GastroPlusTM, J. Pharm. Sci. 108 (1) (2019 Jan) 305–315.

[21] M. Van der Veken, J. Brouwers, A.C. Ozbey, K. Umehara, C. Stillhart, N. Knops, et al., Investigating tacrolimus disposition in paediatric patients with a physiologically based pharmacokinetic model incorporating CYP3A4 ontogeny, mechanistic absorption and red blood cell binding, Pharmaceutics 15 (9) (2023 Sep) 2231.

[22] M. Jamei, B. Abrahamsson, J. Brown, J. Bevernage, M.B. Bolger, T. Heimbach, et al., Current status and future opportunities for incorporation of dissolution data in PBPK modeling for pharmaceutical development and regulatory applications: OrBiTo consortium commentary, Eur. J. Pharm. Biopharm. 155 (2020 Oct 1) 55–68.

[23] M.E.F. Mohamed, S. Trueman, A.A. Othman, J.H. Han, T.R. Ju, P. Marroum, Development of in vitro–in vivo correlation for upadacitinib extended-release tablet formulation, AAPS J. 21 (6) (2019 Oct 25) 108.

[24] G. Lemmens, J. Brouwers, J. Snoeys, P. Augustijns, T. Vanuytsel, Insight into the colonic disposition of celecoxib in humans, Eur. J. Pharm. Sci. 145 (2020 Mar 30) 105242.

[25] FDA, Product Quality Review(s) [cited 2023 Aug 8]; Available from: https://www.accessdata.fda.gov/drugsatfda_docs/nda/2019/211675Orig1s000ChemR.pdf.

[26] F. Kesisoglou, A. Mitra, Application of absorption modeling in rational design of drug product under quality-by-design paradigm, AAPS J. 17 (5) (2015 Sep 1) 1224–1236.

[27] EMA, European Medicines Agency [Cited 2023 Jul 28]. Rinvoq. Available from: https://www.ema.europa.eu/en/medicines/human/EPAR/rinvoq, 2019.

[28] Z. Ni, A. Talattof, J. Fan, E. Tsakalozou, S. Sharan, D. Sun, et al., Physiologically based pharmacokinetic and absorption modeling for osmotic pump products, AAPS J. 19 (4) (2017 Jul 1) 1045–1053.

[29] K.J. Watson, J. Davis, H.M. Jones, Application of physiologically based pharmacokinetic modeling to understanding the clinical pharmacokinetics of UK-369,003, Drug Metab. Dispos. 39 (7) (2011 Jul 1) 1203–1213.

[30] B. Hens, Y. Tsume, M. Bermejo, P. Paixao, M.J. Koenigsknecht, J.R. Baker, et al., Low buffer capacity and alternating motility along the human gastrointestinal tract: implications for in vivo dissolution and absorption of Ionizable drugs, Mol. Pharm. 14 (12) (2017 Dec 4) 4281–4294.

[31] C.L. Li, L.G. Martini, J.L. Ford, M. Roberts, The use of hypromellose in oral drug delivery, J. Pharm. Pharmacol. 57 (5) (2005) 533–546.

[32] E.D. Jorgensen, D. Bhagwat, Development of dissolution tests for oral extended-release products, Pharm. Sci. Technol. Today 1 (3) (1998 Jun 1) 128–135.

[33] F. Franek, P. Holm, F. Larsen, B. Steffansen, Interaction between fed gastric media (ensure plus®) and different hypromellose based caffeine controlled release tablets: comparison and mechanistic study of caffeine release in fed and fasted media versus water using the USP dissolution apparatus 3, Int. J. Pharm. 461 (1) (2014 Jan 30) 419–426.

[34] U. Klančar, B. Markun, S. Baumgartner, I. Legen, A novel beads-based dissolution method for the in vitro evaluation of extended release HPMC matrix tablets and the correlation with the in vivo data, AAPS J. 15 (1) (2012 Nov 28) 267–277.

[35] B. Ramos Pezzini, H. Gomes Ferraz, Bio-dis and the paddle dissolution apparatuses applied to the release characterization of ketoprofen from hypromellose matrices, AAPS PharmSciTech 10 (3) (2009 Sep) 763.

[36] H.D. Williams, K.P. Nott, D.A. Barrett, R. Ward, I.J. Hardy, C.D. Melia, Drug release from HPMC matrices in milk and fat-rich emulsions, J. Pharm. Sci. 100 (11) (2011 Nov 1) 4823–4835.

[37] C. Markopoulos, C.J. Andreas, M. Vertzoni, J. Dressman, C. Reppas, In-vitro simulation of luminal conditions for evaluation of performance of oral drug products: choosing the appropriate test media, Eur. J. Pharm. Biopharm. 93 (2015 Jun 1) 173–182.

[38] S. Klein, The use of biorelevant dissolution media to forecast the in vivo performance of a drug, AAPS J. 12 (3) (2010 May 11) 397–406.

[39] G. Lemmens, J. Brouwers, J. Snoeys, P. Augustijns, T. Vanuytsel, Insight into the colonic disposition of sulindac in humans, JPharmSci 110 (1) (2021 Jan 1) 259–267.